ORIGINAL PAPER

Permafrost-thaw lake development in Central Yakutia: sedimentary ancient DNA and element analyses from a Holocene sediment record

Izabella Baisheva · Luidmila Pestryakova · Sardana Levina · Ramesh Glückler · Boris K. Biskaborn · Stuart A. Vyse · Birgit Heim · Ulrike Herzschuh · Kathleen R. Stoof-Leichsenring

Abstract In Central Yakutia (Siberia) livelihoods of local communities depend on alaas (thermokarst depression) landscapes and the lakes within. Development and dynamics of these alaas lakes are closely connected to climate change, permafrost thawing, catchment conditions, and land use. To reconstruct lake development throughout the Holocene we analyze sedimentary ancient DNA (sedaDNA) and biogeochemistry from a sediment core from Lake Satagay, spanning the last c. 10,800 calibrated years before present (cal yrs BP). SedaDNA of diatoms and macrophytes and microfossil diatom analysis reveal lake formation earlier than 10,700 cal yrs BP. The sedaDNA approach detected 42 amplicon sequence variants (ASVs) of diatom taxa, one ASV of Eustigmatophyceae (*Nannochloropsis*), and 12 ASVs of macrophytes. We relate diatom and macrophyte community changes to climate-driven shifts in water level and mineral and organic input, which result in variable water conductivity, in-lake productivity, and sediment deposition. We detect a higher lake level and water conductivity in the Early Holocene (c. 10,700–7000 cal yrs BP) compared to other periods, supported by the dominance of *Stephanodiscus* sp. and *Stuckenia pectinata*. Further climate warming towards the Mid-Holocene (7000–4700 cal yrs

I. Baisheva · R. Glückler · B. K. Biskaborn · S. A. Vyse · B. Heim · U. Herzschuh · K. R. Stoof-Leichsenring (✉)
Polar Terrestrial Environmental Systems, Alfred Wegener Institute Helmholtz Centre for Polar and Marine Research, Potsdam, Germany
e-mail: kathleen.stoof-leichsenring@awi.de

I. Baisheva
e-mail: izabella.baisheva@awi.de

R. Glückler
e-mail: ramesh.glueckler@awi.de

B. K. Biskaborn
e-mail: boris.biskaborn@awi.de

S. A. Vyse
e-mail: stuart.vyse@awi.de

B. Heim
e-mail: birgit.heim@awi.de

U. Herzschuh
e-mail: ulrike.herzschuh@awi.de

I. Baisheva · R. Glückler · U. Herzschuh
Institute for Environmental Science and Geography, University of Potsdam, Potsdam, Germany

I. Baisheva · L. Pestryakova · S. Levina
Institute of Natural Sciences, North-Eastern Federal University of Yakutsk, Yakutsk, Russia
e-mail: lapest@mail.ru

S. Levina
e-mail: levina_sardan@mail.ru

U. Herzschuh
Institute for Biochemistry and Biology, University of Potsdam, Potsdam, Germany

BP) led to a shallowing of Lake Satagay, an increase of the submerged macrophyte *Ceratophyllum,* and a decline of planktonic diatoms. In the Late Holocene (c. 4700 cal yrs BP–present) stable shallow water conditions are confirmed by small fragilarioid and staurosiroid diatoms dominating the lake. Lake Satagay has not yet reached the final stage of alaas development, but satellite imagery shows an intensification of anthropogenic land use, which in combination with future warming will likely result in a rapid desiccation of the lake.

Introduction

Alaases are thermokarst depressions with meadows (Soloviev 1959) and residual thaw lakes (alaas lakes) which constitute the typical alaas landscape (Bosikov 1991; Crate et al. 2017). Approximately 16,000 alaases are located in the Central Yakutian lowland, covering a total area of 4410 km^2, corresponding to approximately 17–30% of the total land area of the region (Bosikov 1991). Early Holocene warming in Central Yakutia (Biskaborn et al. 2021) led to thermokarst formation due to degradation of the ice wedge complex (Bosikov 1991; Séjourné et al. 2015). Alaases develop in a weakly sloping catchment as closed or semi-closed thermokarst depressions on top of permafrost. The formation of alaases has three main stages: *dyede*, *tyympy,* and a residual lake in the final *alaas* stage (Bosikov 1991). *Dyede* means "rounded lake with low but steep banks, including centered polygons in the bottom". As a term, it was introduced by Soloviev (1959) to characterize the initial stage of alaas development. *Tyympy* is the stage of lake enlargement when underground ice melt results in a drastic increase in the volume of water, and a flattening of the bottom of the basin by sedimentary deposits (Bosikov 1991). In the transition from *dyede* to *tyympy* stages, the formation of a depression with lower elevation occurs. The main source of water for alaas lakes is snowmelt in spring and summer precipitation. In the transition of *tyympy* to the final *alaas* stage, after partial lake water evaporation, a meadow vegetation appears on their banks. These grass-covered alaas basins and the availability of freshwater in remnant lakes make them ideal settlement areas in the

harsh continental climate of Central Yakutia. Alaas lakes are the only sources of water supply for 1/5 of the population of Yakutia (Desyatkin 2004). Development of alaases is a natural process (Soloviev 1959; Bosikov 1991) but intensified agriculture can eventually cause the irreversible loss of alaas lake systems (Desyatkin et al. 2021). Freshwater availability is already a serious concern in Central Yakutia (Herzschuh et al. 2013).

It is important to understand the response of alaas lakes and their ecological condition to a warming climate in the past in order to infer their potential development under continued warming and intensified human usage. The composition of aquatic communities, derived from diatoms and macrophytes, in combination with biogeochemical proxies, derived from X-ray fluorescence (XRF) data, are valuable indicators to reconstruct aquatic diversity changes throughout time and the influence of catchment-related environmental factors.

Important bioindicators of lake-water quality are diatoms (class Bacillariophyceae) and macrophytes (Zhao et al. 2021). Diatoms are one of the most commonly used bioindicators and serve as key indicator organisms in boreal regions (Palagushkina et al. 2012). Diatom assemblages have been shown to be sensitive to hydrochemical parameters, water depth, nutrients, and catchment vegetation around the lake, but also indirectly to atmospheric changes such as air temperature and precipitation (Pestryakova et al. 2018). Microfossil records of diatoms have been used to reconstruct past diatom compositions in Yakutian lake sediments explored by light-microscopy (Pestryakova et al. 2012; Biskaborn et al. 2016) and sedimentary ancient DNA (sedaDNA) metabarcoding for northern lakes (Stoof-Leichsenring et al. 2020). Although submergent macrophytes are valuable indicators of water and nutrient level fluctuations, the sparse fossil record limits investigations on past macrophyte communities, while sedaDNA suitably archives macrophyte DNA from arctic and alpine areas (Alsos et al. 2018; Stoof-Leichsenring et al. 2022) which facilitates paleo-reconstructions. Thus, both diatom and macrophyte sedaDNA records are promising proxies for Central Yakutian lake development.

XRF-derived element ratios and carbon and nitrogen geochemistry are valuable proxies for sedimentary characteristics and biogeochemical properties

in thermokarst-lake sediments helping to decipher catchment-related changes (Bouchard et al. 2011; Biskaborn et al. 2013, 2019; Vyse et al. 2020).

In this study we examine an alaas lake's development through time, exemplified by a sediment core from Lake Satagay, Central Yakutia. We use sedaDNA proxies, targeting diatoms and macrophytes, and XRF data, to reconstruct alaas lake development during the last 10,800 years. We aim to answer the following research questions: (1) How did the aquatic communities of Lake Satagay, exemplified by diatoms and macrophytes, change during the Early, Mid, and Late Holocene? (2) How did catchment-related changes affect lake development and aquatic communities? (3) How is the development of an alaas lake connected to external factors?

Material and methods

Study area

Lake Satagay (N 63.07816°, E 117.99806°) is located in Central Yakutia (Sakha Republic), East Siberia, on the Lena-Viluy terrace, within the catchment of the River Viluy, 805 km west from Yakutsk (Fig. 1a). Permafrost in this region is continuous, with a thickness of c. 400 to 700 m (Fedorov et al. 2018). The climate is characterized as extremely continental with warm summers and very cold, dry winters with a mean annual air temperature ranging between − 11.5 and − 7.5 °C (Fedorov et al. 2018).

In its current state, Lake Satagay is a shallow thermokarst lake within an alaas system (Fig. 1b). There are numerous other alaas landforms close by, with some of them currently used for agriculture (haymaking and cattle and horse pastures). The estimated total area of the alaas system including the lake, wetland, and surrounding grassland is c. 2.5 km^2. Lake surface area is c. 1.7 km^2, estimated from an ESRI © satellite image.

Fieldwork

A sediment core and surface water samples were collected during the Expedition "Chukotka-Yakutia 2018", which was organized and conducted jointly by the Alfred Wegener Institute Helmholtz Centre for Polar and Marine Research (AWI) and the North-Eastern Federal University (NEFU) (Kruse et al. 2019). In early August 2018, the lake's maximum depth was 1.8 m, with a low water transparency of 0.56 m, and high dissolved organic carbon (DOC) concentration of 29.9 mg/L. Sediment core
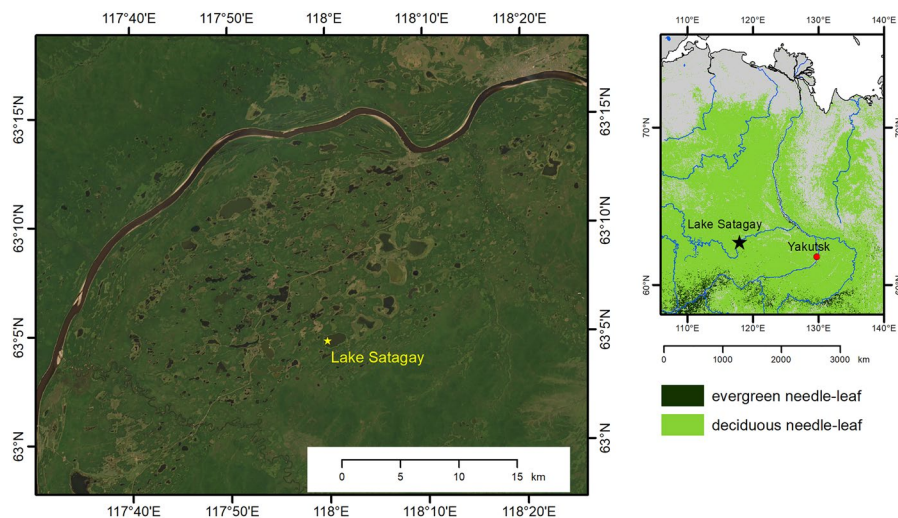

Fig. 1 Lake Satagay study site. **a** Overview map of eastern Siberia, with evergreen and deciduous needle-leaf forest classification (merged together from forest classes of the European Space Agency (ESA) Climate Change Initiative (CCI) Landcover) and the position of the Lake Satagay indicated (black star). **b** Zoomed in map of the Lake Satagay with the position of the core indicated (white star). Background satellite image source: ESRI, Maxar, GeoEye, Earthstar Geographics, CNES/Airbus DS, USDA, USGS, AeroGRID, IGN, and the GIS User Community

EN18224-4, with a diameter of 6 cm and a length of 121 cm, was retrieved using an UWITEC gravity corer with hammer modification from the deepest measured point of the lake (Fig. 1b). Surface water was analyzed in situ with a WTW Multi 340i for pH, conductivity, and oxygen values. Samples from surface water were passed through a cellulose-acetate filter (0.45 μm pore size), and hydrochemical analyses were performed at the laboratories at AWI Potsdam, Germany. Water-chemistry parameters from field measurements together with laboratory results revealed alkaline water with moderate specific conductivity (Table S1).

Laboratory analyses

Sediment core subsampling

Subsampling of the core was performed in a cleaned and cooled chamber at the German Research Centre for Geosciences (GFZ), Potsdam. Core EN18224-4 lacks visible lamination, mostly being a homogeneous, brown color, with only one layer where a brighter shade is present between 42 and 36 cm depth. The core was subsampled at 1 cm intervals and sediment slices were separated into samples for the different analyses, including, for this study, sedaDNA, diatom morphology, and geochemistry.

Dating

The chronology for EN18224-4 is based on radiocarbon age dating of ten bulk sediment samples, spread equally across the core. It indicates continuous sedimentation throughout the last c. 10,800 cal yrs BP covered by the sediment core. A detailed description of the age-depth modelling approach can be found in Glückler et al. (2022). In this study, the mean value of the modelled chronologies per depth, calibrated to calendar years BP, is used. We refer to Walker et al. (2012) for the Holocene zonation, but with the integration of regional climate condition of Central Yakutia (Biskaborn et al. 2012; Ulrich et al. 2017) and the results of this study: Early Holocene (10,700–7000 cal yrs BP) Mid-Holocene (7000–4700 cal yrs BP) and Late Holocene (4700 cal yrs BP—present).

Sedimentology

The sedimentological analytics were performed in the sediment laboratory at AWI Potsdam. For measurement of total organic carbon (TOC), 111 samples, and for total nitrogen (TN) measurement, 17 samples were freeze-dried and homogenized by grinding in a planetary mill. TOC was subsequently measured via loss on ignition in all 111 samples of the sediment core, using a soliTOC cube analyzer (Elementar Analysensysteme GmbH, Germany). Total inorganic carbon (TIC) and TOC are given in weight percentage (wt%). Nitrogen was measured from the 17 freeze-dried samples spread across the core, using a TruMac CNS elemental analyzer (LECO, Germany). Following Meyers (2002), wt% of TOC and TN are used to calculate the C/N ratio, multiplied by the ratio of atomic weights of N–C (1.167) to yield C/N atomic ratios (TOC/TN$_{atomic}$).

XRF scanning

To get high-resolution data on elemental concentrations for the sediment core, one half was scanned using an Avaatech X-Ray Fluorescence Spectrometer (XRF) Core Scanner at the Bundesanstalt für Geowissenschaften und Rohstoffe (BGR), Berlin, Germany. Twenty-four elements were measured to obtain the chemical composition of the core. We performed a 2 mm step scan using 10 kV at 750 μA, 16 s count time without filter for light elements, and 30 kV at 1500 μA with Pd-Thick filter for heavier elements. For this study, we used nine elements (Fe, Mn, Sr, Rb, Si, Al, Ti, Br, and Zr).

Microfossil diatom preparation

Diatom slide preparation for microscopic investigations followed a standard procedure (Battarbee et al. 2001) and was conducted in a dedicated diatom laboratory at AWI Potsdam. Ten samples of 0.5–1.0 g of sediment were freeze-dried to remove all organic material. Samples were cooked at 90 °C in 30% hydrogen peroxide under a fume hood for 7–8 h. Then, hydrochloric acid was added to stop the reaction and remove remaining carbonates. Diatom slides were fixed on a glass slide using a hot plate and Naphrax resin. Diatom counting was performed using a Zeiss Axioscope A1 light microscope with

a Plan-Apochromat 100×/1.4 Oil Ph3 objective at a magnification of 1000x. A minimum of 500 diatom valves were counted for each sample (Pestryakova et al. 2012). Diatom-valve concentration was estimated using a formula from Pestryakova et al. (2016). The number of diatom valves in 1 g of sediment equals the quotient of **bcde** divided by **fgh**, where **b** is dilution; **c** is the number of rows in the cover slips at 100× magnification; **d** is the number of fields in a row; **e** is the number of counted valves, and divisors are: **f** dry sediment; **g** drop volume (Battarbee cup), and **h** number of viewed fields of view. Diatom identification was supported by using established literature (Krammer and Lange-Bertalot, 1986–1991; Lange-Bertalot 1993; Lange-Bertalot and Metzeltin 1996), and an online database was used for synonyms (http://www.algaebase.org). Habitat classification is based on Pestryakova et al. (2012, 2016, 2018).

SedaDNA approach

SedaDNA was obtained from 65 core sediment samples. DNA extractions were performed following Epp et al. (2019) using either the Dneasy PowerSoil DNA Isolation Kit (Qiagen, Germany) with 250 mg sediment input, or the Dneasy PowerSoil Max DNA Isolation Kit (Qiagen, Germany) with about 1.0–2.4 g sediment input. Samples were extracted twice to realize a total sediment input of 500 mg. A few samples needed to be extracted four times (4×250 mg) to gain enough DNA for polymerase chain reaction (PCR) amplification. For each extraction batch one blank was added to control for putative contamination in the DNA extraction chemicals.

Combining and concentrating of extracted sedaDNA was realized with the GeneJet PCR purification Kit (Thermo Scientific, USA). Concentrated DNA was quantified with a broad range dsDNA Assay Qubit Fluorometer (Invitrogen, USA). The PCR set-up included 3 μL of extracted sedaDNA (diluted to 3 ng μL⁻¹), primers (1 μL each), 0.25 μL of Platinum™ Taq High Fidelity DNA Polymerase and buffer (Invitrogen, USA), 10×HiFI buffer (2.5 μL), dNTPS (2.5 μL), Bovine Serum Albumin (1 μL; VWR, Germany), MgSO4 (1 μL), and 12.75 μL of DEPC water (VWR, Germany). Primers for the amplification of diatoms targeted a diagnostic short diatom metabarcode (primers: diat_rbcL705 and diat_rbcL808; Stoof-Leichsenring et al. 2012). For

plant DNA metabarcoding we used standard primers targeting the chloroplast trnL P6 loop (Taberlet et al. 2007). All primers were modified with an NNN-8 bp tag to establish sample multiplexing. All steps from DNA extraction down to PCR-set-up were performed in a dedicated paleogenetic laboratory at AWI Potsdam.

PCRs for diatom and plant metabarcoding were run in three replicates along with No Template Controls (NTCs) to control chemical contamination of PCR chemicals. PCR products were amplified in a Biometra ThermoCycler (Biometra, Germany) at initial denaturation at 95 °C for 5 min, followed by PCR cycles with denaturation at 95 °C for 30 s, annealing at 50 °C for 30 s and elongation at 68 °C for 30 s. For the amplification of diatom DNA, we used 50 cycles, while 40 cycle PCRs were run for the amplification of plant DNA. Each PCR product had been checked by running gel electrophoresis in 2% agarose gel and displaying bands in UV (Jena Analytics).

Purification of PCR products for each sample was done with MinElute (Qiagen, Germany), following the manufacturer's protocol. The first pool contained 3×61 PCR products from plant DNA amplifications. The second pool contained 3×65 PCR products from diatom DNA. Pooled samples were prepared with a PCR-free library (metafast protocol) and sequenced in paired-end mode (2×150 bp) on an Illumina NextSeq 500 platform (Illumina Inc.) at the external sequencing service (Genesupport, Fasteris SA, Switzerland).

Sequence-data processing and filtering

After Illumina sequencing, data were processed using OBITools3 (https://git.metabarcoding.org/obitools/obitools3). A general description of the bioinformatic pipeline is given in Boyer et al. (2015). To align forward and reverse reads, data were combined using the "*obi alignpairedend*" command, and to remove unpaired reads "*obi grep*" was used. To allocate reads to the corresponding combinations of primer tags the command "*obi ngsfilter*" was used. Grouping and counting of identical sequences was performed using "*obi uniq*". Denoising data using "*obi annotate*" removed sequences with < 10 counts and < 10 length. The taxonomic assignment was conducted by using different databases. Diatom and plant EMBL reference databases were built by applying "*obi ecopcr*" with diatom and plant primers, respectively, on the

EMBL Nucleotide Sequence Database (Release 143, April 2020). Ecopcr results were then converted with "*build_ref_db*" into an ecopcr database that "*obi eco-tag*" uses for taxonomic classification.

Plant DNA sequences were matched against the EMBL Nucleotide Sequence Database and the Arctic and Boreal vascular plant and bryophytes database (Sønstebø et al. 2010; Willerslev et al. 2014; Soininen et al. 2015) for plants. Only 100% matches with either the Arctic or EMBL database were considered. If Arctic and EMBL matches both showed 100%, the taxonomic name from the Arctic database was selected. Results from the OBITools pipeline of the diatom dataset were further filtered at the level of amplicon sequence variants (ASVs). The taxonomic assignment was based on 98–100% similarity to at least one entry of the EMBL reference database. ASVs not belonging to Bacillariophyta (diatoms) were discarded. ASVs were assigned "Scientific names" (to the best possible assignment which can vary between family, genus, or species level). Final count data were resampled (https://github.com/StefanKruse/R_Rarefaction) to the minimum number of counts (n = 2050, derived from 65 samples) to normalize the dataset prior to subsequent statistical analyses. This process was repeated 100 times and the mean value calculated. The final dataset includes 422 ASVs, which are grouped into 43 unique "Scientific names".

Results from OBITools3 pipeline of the plant dataset were further filtered and aggregated at the best scientific name level. Terrestrial plants were excluded and aquatic plant data were resampled to the minimum number of counts (n = 1653, derived from 61 samples). This process was repeated 100 times and the mean value calculated. The final dataset consists of 14 unique taxa, including ten submergent plant types and two emergent macrophytes. In addition, four cyanobacterial taxa were identified with the plant metabarcoding approach and were kept in the dataset.

Statistical analyses

All statistical analyses and visualizations were completed in R v. 3.6.1 (R Core Team 2019). Elemental compositional data from XRF scanning are given in counts per second (cps). Single element values were transformed with a centered-log ratio (clr) transformation, while for ratios of elements, an additive-log ratio (alr) transformation was applied (R package "compositions"; van den Boogaart and Tolosana-Delgado 2006). Ages were extrapolated using "na. approx" (R package "stats") for the high-resolution XRF data, in order to run pairwise correlation and PCA. Two gaps in the TOC and TIC data were linearly interpolated using the "approx" function (R package "stats"). Pearson correlation analysis was performed on sedimentological and geochemical variables to test for correlation between the elements and the element ratio data with TOC, TIC, and the TOC/TN$_{atomic}$ ratio.

Bar plots of taxa were produced for sedaDNA and the microscopic diatom datasets using the strat. plot function from the rioja R-package (Juggins 2019). Relative abundance from resampled counts of sedaDNA diatoms and macrophytes as well as of diatoms was calculated for CONISS clustering and evaluated by the "broken stick" model in R (packages "vegan", Oksanen et al. 2015, and "rioja"; Juggins 2019). The number of zones was defined by a dispersion value higher than the random broken-stick model.

Principal component analysis (PCA) was used to illustrate the compositional change in a combined dataset, including of diatoms and macrophytes, the impact of selected sedimentological and geochemical as explanatory variables for community changes. Therefore, log-transformed relative proportions for sedaDNA data and selected clr and alr transformed XRF and square-rooted TOC and TIC values were plotted via "envfit" onto the PCA ordination calculated with the "rda" function. RDA (redundancy analysis) using the function "rda" was applied to calculate the single and unique (using the function "Condition") proportion of explained variance. Additionally, we calculated the proportion of all significant explanatory variables and by using the function "ordistep" (direction = forward selection) an automatic search that maximizes the R^2 in order to select the best explanatory variables. The function "RsquareAdj" calculates the adjusted R using a permutation approach. All steps of the ordination analyses were performed with the "vegan" R-package (Oksanen et al. 2015).

Results

Sedimentological and geochemical temporal stages of the lake

The sediment core EN18224-4 is characterized by a stable sedimentation rate (mean of 0.14 ± 0.09 mm year^{-1}), with one exception in the period between 4500 and 5500 cal yrs BP, where the sedimentation rate increases to 0.42 mm year^{-1} (Glückler et al. 2022).

TOC gradually increases during the Early Holocene (from 17.7 to 39.5 wt%) and from 6000 cal yrs BP to recent it stays high (mean value 43.3 wt%; Fig. 2), except between 5000 and 4300 cal yrs BP, when TOC values abruptly decrease to 21.8 wt% (at c. 4900 cal yrs BP). TIC in the Early Holocene from c. 10,500 to 9700 cal yrs BP is relatively high (mean 0.9 wt%), then decreases gradually and stays relatively low in the Mid-Holocene (mean of 0.08 wt%). The highest TIC is between c. 4900 and 4700 cal yrs BP in the Mid-Holocene.

Values of TOC/TN$_{atomic}$ range from 8.4 to 14.9. In the Early Holocene, the TOC/TN$_{atomic}$ maximum is 14.9 (at 10,789 cal yrs BP) and the minimum is 10.8 (at c. 9000 cal yrs BP). Values are stable in the Mid-Holocene, ranging from 11.6 to 10.5. One peak occurs in the Late Holocene (13.0; c. 4900 cal yrs BP) before it abruptly decreases to 8.4 (c. 4200 cal yrs BP).

The Sr/Rb shows two peaks at c. 5100 cal yrs BP (5.1) and at c. 4740 cal yrs BP (5.3). An initial period of increase runs from c. 10,830 cal yrs BP to 8860 cal yrs BP. After this period, the Sr/Rb of c. 4.0 gradually decreases down to 1.6 at around 6140 cal yrs BP. The ratio shifts to a second period of increase until c. 4740 cal yrs BP and then decreases until 600 cal yrs BP. The Mn/Fe increases in the Early Holocene and through the Mid-Holocene towards a maximum of -1.6 in the Late Holocene at c. 3790 cal yrs BP. Then Mn/Fe decreases to a minimum of -4.4 at c. 820 cal yrs BP. The Si/Al has lowest values of around 2.6 in the Early Holocene between 10,830 to 10,280 cal yrs BP. The Si/Ti is rather stable with a mean around 0.6. Relatively higher values occur only between 4970 and 4640 cal yrs BP. The Br shows a peak at c. 9870 cal yrs BP (-0.2) and a second at c. 6960 cal yrs BP (-0.4). The Zr is high at around 0.2 in the period between c. 10,830 and 9790 cal yrs BP, while its overall mean is -0.36.
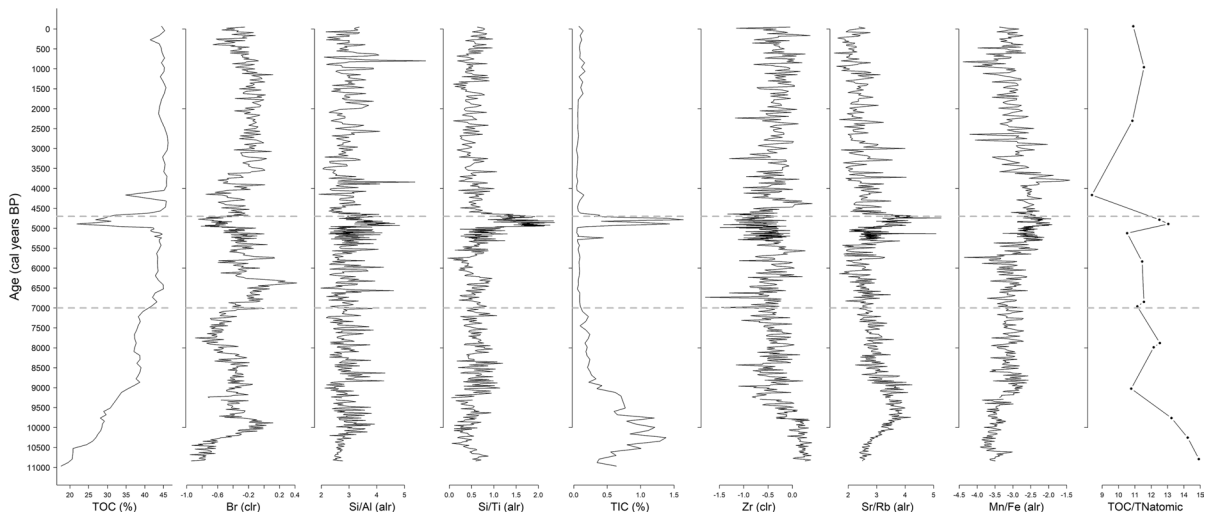

Fig. 2 Vertical profile of selected XRF elements and ratios (centered-log ratio (clr) and additive-log ratio (alr) transformed and smoothed) and concentrations of total organic carbon (TOC (wt%)) and total inorganic carbon (TIC (wt%)) and distribution of TOC/TN$_{atomic}$ ratio over time. Grey dashed lines divide the core into Early, Mid, and Late Holocene.

Compositional turnover in diatoms

Diatom composition derived from the sedaDNA metabarcoding approach

Our raw data comprises a total of 13,028,150 counts and 2311 ASVs. After filtering for 98–100% similarity to the reference database, 9,895,410 counts remained. Of these, 90.05% is assigned to Bacillariophyceae (diatoms; 8,991,139 counts), 9.93% to Eustigmatophyceae (*Nannochloropsi*s; 982,918 counts), and 0.01% to Heteropediaceae (900 counts) and Kryptoperidiniaceae (86 counts), while 367 counts were sequenced from blanks and NTCs. As diatoms and *Nannochloropsis* are phylogenetically placed within the group of Stramenopiles, *Nannochloropsis* was kept. We discarded Heteropediaceae, Kryptoperidiniaceae, blanks, and NTCs in a further filtering step. The final dataset contains 9,894,057 reads (75.95% of raw total reads) and aggregates to 422 unique ASVs. Rarefaction to minimal counts (n = 2050) decreased the dataset to a total count of 129,150. After filtering and resampling, two samples were discarded. 422 ASVs were grouped into 43 taxa names, of which 42 taxa cover different

levels of taxonomy within Bacillariophyceae, and one taxon of Eustigmatophyceae (Fig. 3).

Twenty-eight ASVs (69.2% of rarified dataset) were identified to species level (species *Amphora copulata, Aulacoseira granulata, Cocconeis placentula, Cymbella heterogibbosa, Cymbopleura naviculiformis, Epithemia sorex, Fragilaria construens, Gomphonema carolinense, Lindavia radiosa, Navicula radiosa, Neidium fossum, Nitzschia* cf. *pusilla, Nitzschia draveillensis, Nitzschia palea, Pinnularia brebissonii, Pseudostaurosira elliptica, Sellaphora bacillum, Sellaphora laevissima, Stauroneis phoenicenteron, Urosolenia eriensis,* plus eight unclassified: *Navicula* sp.AT-201Gel01, *Navicula* sp.ETS07, *Navicula* sp.KEL-2015, *Staurosirella* sp.1LKM-2011, *Synedra* sp.KEL-2015, unclassified *Pinnularia,* unclassified *Staurosira,* unclassified *Stephanodiscus*), nine ASVs (13.3% of rarified dataset) to genus (*Achnanthidium, Eolimna, Gomphonema, Neidium, Nitzschia, Pinnularia, Sellaphora, Stephanodiscus, Ulnaria*), and five ASVs (0.5% of rarified dataset) to family (Achnanthidiaceae, Cymbellaceae, Fragilariaceae, Rhopalodiaceae, Stephanodiscaceae). The final taxonomically rarified dataset includes 18 families, 24 genera, and 28 species. The Eustigmatophyceae ASV has been
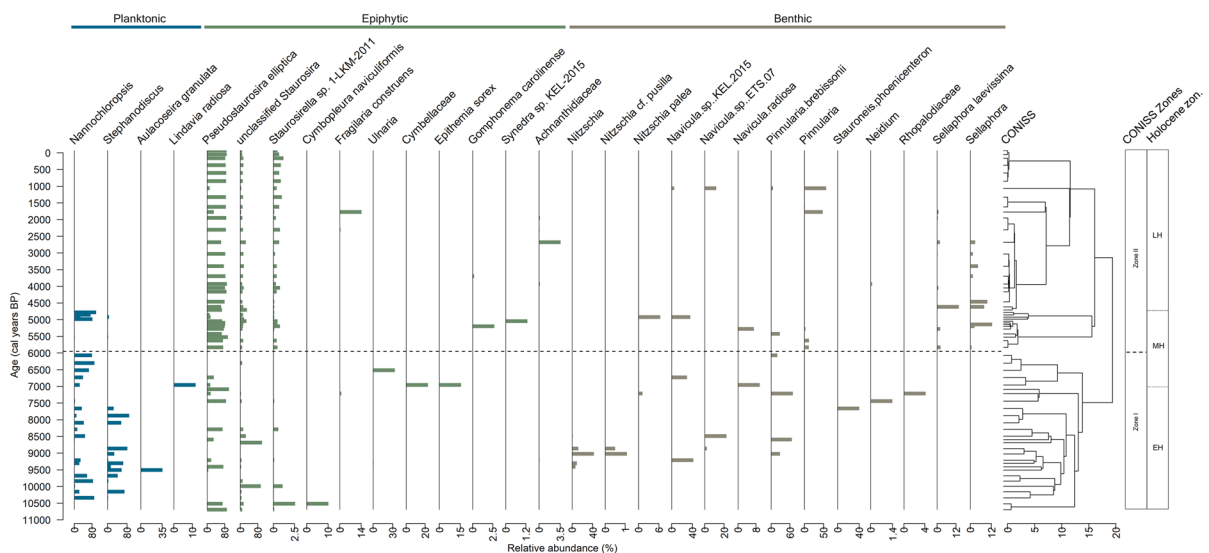

Fig. 3 The stratigraphic diagram shows the relative abundance (%) of diatom taxa and *Nannochloropsis* derived from the metabarcoding approach. Clustering was established with CONISS, with zones indicated by the black dashed line and the box on the right. Holocene zonation for the core is given in the right-hand box, *EH* Early Holocene, *MH* Mid-Holocene, *LH* late Holocene. Only taxa with abundances ≥ 1% are shown. Blue bars indicate planktonic diatoms and *Nannochloropsis,* green bars indicate epiphytic diatoms, and brown bars indicate benthic diatoms. Note the different scales of relative abundance

identified to genus level of planktonic *Nannochloropsis*, which comprises 16.9% of the rarified dataset. A further 9.5% of rarified ASVs correspond to planktonic diatoms and 73.6% to benthic diatoms.

CONISS clustering divided the diatom record into two zones. Zone I covers the period between 10,700 and c. 5800 cal yrs BP, and thus spans from the Early Holocene to the first half of the Mid-Holocene. Zone II stretches from the second half of the Mid-Holocene (c. 5800 cal yrs BP) through the whole Late Holocene until the present day. Diatom richness varies from 30 taxa that were detected in the Early Holocene, to 23 in the Mid-Holocene (7000–5000 cal yrs BP), and 31 taxa in the Late Holocene.

In general, *Pseudostaurosira elliptica* (27.8%), *Stephanodiscus* (23.5%), and *Nannochloropsis* (20.5%) are dominant within zone I, whereas unclassified *Staurosira* (13.5%) is subdominant. However, in the Early Holocene (10,700–c. 7600 cal yrs BP) there are some interchangeable shifts of the ascendancy between dominant and subdominant taxa. After an abrupt extinction of *Stephanodiscus* (no reads), *Pseudostaurosira elliptica*, unclassified *Staurosira*, *Ulnaria*, and *Pinnularia brebissonii* alternately share dominance. In zone II, a shared dominance of *Pseudostaurosira elliptica* and *Nannochloropsis* is indicated at the end of the Mid-Holocene, while unclassified *Staurosira* remains subdominant. *Stephanodiscus* ASVs indicate a relatively small occurrence in zone

II. Zone II displays a drastic decrease of planktonic diatom abundance when compared to zone I.

Diatom composition derived from the microscopic approach

The number of counted diatom valves in each of ten microscopic samples ranges from 517 to 722 valves/sample (mean=576). Mean diatom concentration per 1 g of sediment is 1.41×10^6. The highest concentration (3.59×10^6 per 1 g of dry sediment) is found in a Mid-Holocene sample (48 cm depth, c. 5000 cal yrs BP), whereas the lowest concentration (0.19×10^6 per 1 g of dry sediment) is from an Early Holocene sample (c. 9300 cal yrs BP). Diatom-valve concentration per 1 g of dry sediment is higher in the Mid-Holocene (mean 2.83×10^6) compared to the Late Holocene (0.69×10^6) and the Early Holocene (1.28×10^6). In total, 38 diatom taxa were detected, including seven taxa identified to genus level and 31 to species level (Fig. 4). Taxonomically, the final fossil diatom dataset includes 16 families, 23 genera, and 31 species.

The most prominent species are epiphytic (84% of the whole dataset): *Staurosira venter* (corresponding to 27%), *Pseudostaurosira brevistrata* (26%), and *S. construens* (13%). The most abundant planktonic diatom, *Fragilaria capucina*, comprises 8% of the whole dataset, while other representatives such as *Aulacaseira ambigua*, *Cyclotella radiosa*,
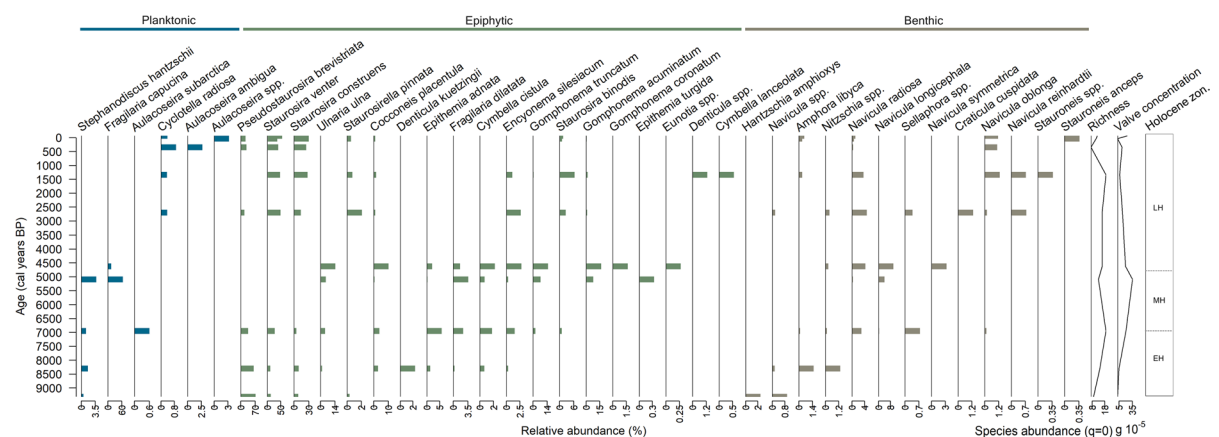

Fig. 4 Relative abundance (%) of diatom taxa in the assemblages gained from morphological identification. Total species richness and valve concentration are given on the right-hand side before the Holocene zonation for the core (EH: Early Holocene, MH: Mid-Holocene, LH: Late Holocene). Blue bars indicate planktonic diatoms, green bars indicate epiphytic diatoms, and brown bars indicate benthic diatoms. Note the different scales of relative abundance

and *Stephanodiscus hantzschii,* comprise only 2% of the dataset. Benthic species comprise only 6% of the whole dataset. *Stephanodiscus hantzschii* was detected only in samples from the early and Mid-Holocene.

Macrophyte composition derived from the sedaDNA metabarcoding approach

Metabarcoding of aquatic plants from Lake Satagay revealed 12 ASVs, whereof ten were assigned to submergent plants and two to emergent plants. Submergent taxa include one ASV assigned to Ceratophyllaceae (68.1%), six ASVs to Potamogetonaceae (30.4%), one ASV assigned to Zannichelliaceae (0.04%), and two ASVs to Haloragaceae (0.6%). The emergent aquatic plants assigned are Menyanthaceae and Typhaceae (0.3%). Along with these macrophytes, four cyanobacterial ASVs assigned to *Planktothrix* and *Dolichospermum crassum* were identified (0.5%).

A CONISS clustering on aquatic plants and cyanobacteria data separates the core into four zones (Fig. 5). Zone I (10,700–9300 cal yrs BP) is dominated by *Potamogeton perfoliatus* and *Stuckenia pectinata* as well as the occurrence of cyanobacteria

Planktothrix and *Dolichospermum crissum*. Zone II (c. 9300 to 7200 cal yrs BP) is characterized by *Potamogeton*, *Stuckenia pectinata,* and *Ceratophyllum demersum*, which is the predominant type from 7200 cal yrs BP up to recent times. In zone III (c. 7200–2700 cal yrs BP) only occasionally are *Potamogeton*, Menyanthes and Nymphaeaceae found in the aquatic plant community. In zone IV (c. 2700 cal yrs BP to present), in addition to the dominant *Ceratophyllum* type, *Myriophyllum sibiricum* and *Potamogeton praelongus* reach higher abundances.

Diatom and macrophyte communities and its relationship with sedimentological and geochemical data

The PCA biplot of the first and second principal components (PC) explain 31.5% and 14.3%, respectively, of the variance in the combined sedaDNA dataset of diatoms, including *Nannochloropsis* and macrophytes (Fig. 6). The ordination separates Mid-Holocene from Early and Late Holocene samples. Variables of environmental data show high association of Mn/Fe, TOC and TIC along the PC1 axis and Zr along the PC2 axis. A dominance of *Ceratophyllum demersum* is associated with high Mn/Fe ratios, whereas a
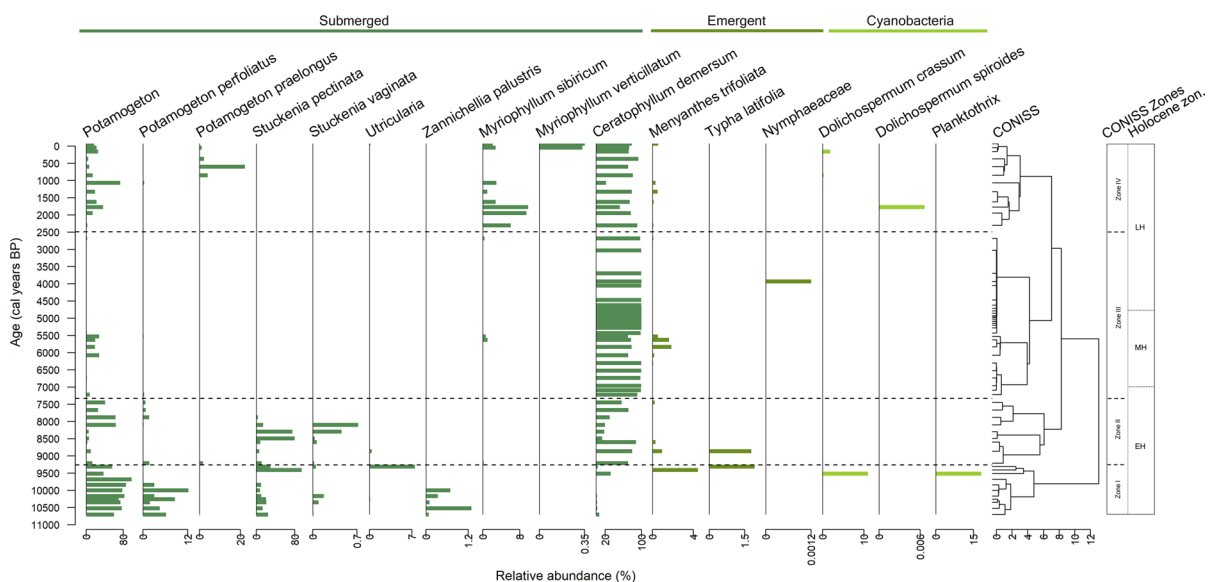

Fig. 5 Relative abundance (%) of sequenced aquatic plants and cyanobacteria. Clustering was established with CONISS, with zones indicated by the black dashed line and on the right. Holocene zonation for the core is given in the right-hand box

EH Early Holocene, *MH* Mid-Holocene, *LH* late Holocene. Dark green bars indicate submergent macrophytes, green bars emergent aquatic plants, and light-green bars cyanobacteria. Note the different scales of relative abundance

Fig. 6 Biplot showing the results of the principal component analysis (PCA) performed on the most dominant sedaDNA diatom taxa and *Nannochloropsis*, indicating their relation to physicochemical variables within Holocene zones (numbers next to sample points refer to their age in cal yrs BP)

dominance of *Potamogeton* is associated with high Zr values. *Stephanodiscus, Potamogeton perfoliatus, Stuckenia pectinata* are associated with high TIC values. Results of the ordistep analyses reveal that TIC, Mn/Fe and Zr are the most important explanatory variables for the diatoms and macrophytes composition. All variables together explain 22.8% of the variance in the combined diatoms and macrophytes dataset ($p < 0.001$). Results for the single explanatory variables are summarized in Table S2.

Discussion

Lake deepening in the early Holocene (10,700–7000 cal yrs BP)

We infer that the thermokarst processes leading to the formation of Lake Satagay were likely initiated in the late glacial and that the lake already existed at the beginning of the Early Holocene. This is supported by the presence of typically cold-adapted

freshwater diatoms and submergent aquatic plants detected in the oldest sample (10,700 cal yrs BP) of the sediment core (Fig. 3). In addition, the presence of algal cells in non-pollen palynomorphs also suggests freshwater conditions already in the Early Holocene (Glückler et al. 2022). This is in accordance with other paleolimnological studies from the Viluy region, which infer that thermokarst development in Central Yakutia began either during the Allerød oscillation (c. 13,500–12,500 cal yrs BP; Andreev 2000), or since the late glacial (c. 12,000 cal yrs BP; Crate et al. 2017). Given the existence of pioneering small benthic fragilarioid taxa, the lake was shallow at the very beginning of the Early Holocene and would thus freeze to the bottom. Similar conditions are seen from the initial formation of other thermokarst lakes in the region (Biskaborn et al. 2012). Biskaborn et al. (2012) suggest that a combination of small benthic fragilarioid taxa together with low TOC and low diatom concentration is indicative of a colder lake environment with extended seasonal ice cover. Lake Satagay's existence and shallow depth in the Early

Holocene (c. 10,700–10,300 cal yrs BP) are further indicated by a positive correlation ($r=0.55$; Figure S3) between TOC and Br such as for the glacial Lake Ilirney in Chukotka (Vyse et al. 2020) both suggesting low productivity. In addition, relatively low Si/Al ratios indicate low productivity (Vyse et al. 2020), with relatively high detrital input indicated by Zr values (Biskaborn et al. 2021). These conditions of low productivity and relatively high detrital input fit well to the initial *dyede* stage of alaas lake development (Bosikov 1991; Fedorov 2022).

Our data suggest deepening of Lake Satagay during the Early Holocene (c. 10,300–10,000 cal yrs BP). At this time, a deepening in the *dyede* stage is possible as the upper layer of the ice complex thaws with high potential for thaw subsidence (Ulrich et al. 2017). We assume that the high values of the Sr/Rb ratio detected in the Lake Satagay record during this time could indicate terrestrial input of larger grain-size particles (Biskaborn et al. 2013, 2021).

The main evidence for a deeper lake during this time is given by the dominant planktonic diatom ASVs of *Stephanodiscus* and *Aulacoseira granulata* that occurred in highest abundance in the Early Holocene (Fig. 3). *Stephanodiscus hantzschii,* for example, has been verified as an indicator species for alaas lakes and is known to occur in magnesium-rich and highly mineralized waters (Pestryakova et al. 2012). The maximum growth rate of *Stephanodiscus* occurs at c. 5 ± 6 °C water temperature in nutrient-rich conditions under ice (van Donk & Kilham 1990). The occurrence of planktonic and under-ice taxa indicate that Lake Satagay was thus deep enough not to freeze down to the bottom completely, as is known to happen to shallow thermokarst lakes during long and cold winters (Pestryakova et al. 2012). Concurrent with *Stephanodiscus* ASVs, are ASVs of the planktonic microalgae *Nannochloropsis*. *Nannochloropsis limnetica*, for example, is known from freshwater/brackish habitats (Krienitz et al. 2000) and can survive under ice (Fietz et al. 2005) and outcompete *Stephanodiscus* (Marzetz et al. 2017). However, the morphological dataset does not fully support the findings of the genetic dataset. In particular, *Stephanodiscus hantzschii* is not the dominant taxon in the Early Holocene samples; *Pseudostaurosira brevistrata* is instead. Further, the submergent macrophyte *Potamogeton perfoliatus,* which grows at a water level optimum between 2.5 and 3 m, supports the inference of deeper water conditions in Lake Satagay during the Early Holocene.

More evidence of a prevailing input of terrestrial plant material is provided by the relatively high TOC/TN$_{atomic}$ ratio in this period (Meyers and Teranes 2002; Biskaborn et al. 2013). A pollen-based vegetation reconstruction by Glückler et al. (2022) reveals open woodlands with extensive grasslands, while charcoal particles reveal increased wildfire disturbances until 8500 cal yrs BP. Potentially, any post-fire thermokarst activity may have contributed to this increase of erosional input (Jones et al. 2015). In addition, the occurrence of warmer periods known from the detection of *Pinus* pollen in lake sediment cores from Central Yakutia at about 9600 cal yrs BP (Andreev et al. 1992) likely accelerated thermokarst processes in the Early Holocene and Lake Satagay seems to have shifted to a deeper *tyympy* stage lake after c. 10,000 cal yrs BP until 8000 cal yrs BP.

With rising temperatures after c. 8000 cal yrs BP (Andreev et al. 1992) the lake was likely exposed to intensified evaporation in dry summers. A putative lake shallowing at the end of the Early Holocene along with a high specific conductivity regime in the lake are supported by the presence of the submergent *Stuckenia pectinata*. This taxon grows in shallow water (0.2–2.0 m; Kipriyanova et al. 2017) and forms large and dense shrubs in brackish lakes with high levels of water conductivity (Herzschuh et al. 2010).

High lake productivity in the Mid-Holocene (7000–4700 cal yrs BP)

Mid-Holocene warming was marked by the establishment of modern-like taiga vegetation after c. 7000 cal yrs BP (Müller et al. 2009). During the Holocene Thermal Maximum (HTM) in Central Yakutia (c. 7000–5000 cal yrs BP) an acceleration of thermokarst processes is assumed (Ulrich et al. 2017). Similar warmer temperatures are reported from Lake Temje between c. 6700 and 4800 cal yrs BP (Nazarova et al. 2013). Warmer HTM temperatures most likely led to a reduction in the ice-covered periods of Lake Satagay, as supported by higher values of the commonly used proxy for lacustrine redox conditions Mn/Fe and increased lake productivity indicated by Br (Vyse et al. 2020).

In the transition from the Early Holocene to the Mid-Holocene both diatom approaches reveal a

compositional change. In the metabarcoding data, Cymbellaceae, *Epithemia,* and *Navicula radiosa* occur. High abundances of *Stauroneis phoenicentron* and *Navicula radiosa,* also seen in the microscopic approach, are indicative of an assumed intermediate lake specific conductivity (100–500 μS cm^{-1}; Pestryakova et al. 2018) throughout this period. We assume the lower specific conductivity and lake shallowing resulted in a significant loss of *Stephanodiscus* and its displacement by the highly productive phytoplankton *Nannochloropsis* (Krienitz et al. 2000; Marzetz et al. 2005) at the beginning of the Mid-Holocene. A scarce occurrence of *Stephanodiscus* has also been attributed to lake shallowing in another study from Sysy-Kyuele, a thermokarst lake in northern Yakutia (Biskaborn et al. 2012). Also, the increase of larger epiphytic diatoms, such as *Gomphonema*, *Ulnaria,* and *Fragilaria dilatata* is known from another Mid-Holocene microfossil record from Lake Boguda (Pestryakova et al. 2012). The detection of larger diatoms, peak values of biogenic silica, Si/Ti and Si/Al ratios, and total valve concentration (2.8×10^6 g^{-1}) can be indicative of a generally high primary productivity. High primary productivity of diatoms is thus likely to increase the sedimentation rate which peaks between c. 5500 and 4500 cal yrs BP in Lake Satagay. Similarly, biological diversification and increased bioproduction is indicated from Lake Sysy Kyuele at around 5700 cal yrs BP (Biskaborn et al. 2012).

The diversity of macrophytes is dominated by *Ceratophyllum demersum* during the Mid-Holocene. Interestingly, *Ceratophyllum demersum* is known to reduce water mixing and increase water clarity through allelopathy (Gross et al. 2003). This phenomenon is characterized by the excretion of substances inhibiting algae growth, which might have caused the abrupt disappearance of *Nannochloropsis* between c. 6000 and 5000 cal yrs BP. Also, algae among the non-pollen palynomorph data decrease after c. 5100 cal yrs BP (Glückler et al. 2022), while pine trees spread rapidly during that time, forming a dense forest which increases water consumption and limits water supply to the lake, causing continuous lake shallowing. Furthermore, forest cover leads to a high allochthonous organic input to the lake, leading to higher DOC concentrations than e.g. in tundra environments (Duff et al. 1998; Dulias et al. 2017). High DOC in the lake considerably reduces water transparency that impacts

the diatom composition (Pienitz and Smol 1993; Saulnier-Talbot et al. 2003; Huang et al. 2020).

Towards the end of the Mid-Holocene there is a pronounced drop of TOC at c. 4900 cal yrs BP, which could be connected to a high sedimentation rate (Glückler et al. 2022). An increase in sedimentation rate could be caused by the erosion of an activated thaw slump during activity triggered by permafrost thaw (Sejourne et al. 2015). Thaw slumping occurred in the *tyympy* stage may lead to the transition from this stage to the next, because it leads to the filling of a lake basin with sediment. This gradually transforms any remaining steep shoreline of the *tyympy* into the gentle slopes of the resulting *alaas* basin. Our results show a peak of TIC and Sr/Rb erosional input proxies indicating lake-basin infilling with sediments and therefore further shallowing of the lake. Moreover, in shallow lakes the limited water depth is another important factor regulating diatom composition (Dulias et al. 2017). Shallow lakes are prone to freeze in winter (Pestryakova et al. 2012). Diatom composition in this extreme condition is mentioned above and in Biskaborn et al. (2012). Indeed, the low depth could have caused the significant decrease of planktonic diatoms and *Nannochloropsis* after c. 4700 cal yrs BP.

Stabilization of a shallow lake system in the Late Holocene (4700 cal yrs BP–present)

The Late Holocene is characterized by a general cooling of the climate. Paleolimnological data from Central Yakutia indicate a decline in temperature after about 4700 cal yrs BP (Nazarova et al. 2013). Our data indicate an overall lower lake productivity compared to the Mid-Holocene. The overall reduction of thermokarst processes due to this cooling trend and the presence of macrophytes may be responsible for the oligotrophic water conditions during the Late Holocene. In addition, previous lake shallowing in the warmer Mid-Holocene and cooler conditions in the Late Holocene, which potentially allowed the lake to freeze down to the bottom, resulted in a change from planktonic to smaller benthic diatoms.

Similar findings of an abrupt decrease in planktonic diatoms, such as *Aulacoseira italica* (c. 4200 cal yrs BP), are recorded from another lake named

Satagay in the Viluysky District by microscopic diatom inspection (Pestryakova et al. 2012).

Both approaches of diatom analyses in our study reveal that there were similar lake conditions at the beginning of the Early Holocene and in the Late Holocene, as shown by the occurrence of smaller fragilarioid types. These include *Staurosira venter*, *S. construens*, and *Pseudostaurosira brevistrata*. Small benthic fragilarioid taxa prefer oligotrophic–neutral to alkaline lakes and can withstand rather unstable environmental conditions, such as caused by annual freezing to the bottom or by flooding, which are common characteristics in permafrost-affected taiga lakes in Central Yakutia (Pestryakova et al. 2018). Prevailing abundance of epiphytic diatoms in the reconstructed diatom composition of the Late Holocene may hint at decreasing lake depth and also at decreasing light availability by the increase of allochthonous DOC due to forest-cover establishment in the lake catchment.

Ceratophyllum demersum is the only macrophyte type at the beginning of the Late Holocene, warmer conditions since c. 2500 cal yrs BP facilitated the growth of *Myriophyllum sibiricum* and *Potamogeton*. This community shift is likely linked to further lake shallowing during the Late Holocene. Other study sites in Central Yakutia indicate a development towards the final *alaas* stage at about 6350–5870 cal yrs BP (Ulrich et al. 2017), resulting in a smaller residual lake in the deepest part of the alaas basin. To date, Lake Satagay has not yet reached the final *alaas* stage with alaas basin drying. The Sr/Rb ratio, since the beginning of the Late Holocene, has decreased towards the present, suggesting reduced thermokarst erosion and thaw-slumping activity similar to processes that are described in Biskaborn et al. (2013) for a thermokarst lake in Northern Yakutia.

Anthropogenic usage of Lake Satagay

Alaas landscapes have a strong cultural relevance, and the alaas basins in particular are subjected to human activities (Pestryakova et al. 2012; Desyatkin et al. 2021). "Satagay" in the Sakha language means "unsettled" or "unresolved". On satellite images from ESRI Satellite ArcGIS/World Imagery (dated to 29/07/2017) we detected no development of grassland around Lake Satagay and thus no visible active agricultural use of the lake so far. However, the existence of several paths through the forest indicate that the lake is used, either as a drinking water source, or as a fishing and/or hunting lake. Since Lake Satagay is located in a basin, the lack of a natural outflow contributes to waterlogging, decreasing its chances of drying out and developing into a final alaas. However, the satellite imagery revealed a 1 km long canal that was dug from the eastern end of Lake Satagay alaas. Most likely this canal is used to control the water level of the neighboring Lake Mongus and could artificially cause accelerated drying of Lake Satagay. Studies from alaases in Central Yakutia, east of the Lena River (Lena-Amga interfluve), reveal that lake cessation takes c. 1500–2000 years (Ulrich et al. 2017), allowing for the higher evaporation of that region (Kumke et al. 2007).

Conclusions

The multi-proxy record from Lake Satagay exemplifies a climate-dependent thermokarst and alaas lake development in Central Yakutia since the Early Holocene. The paleolimnological reconstructions are mainly based on sedimentary ancient DNA (sedaDNA) targeting diatoms and *Nannochloropsis*, as well as macrophytes to characterize the turnover of aquatic communities during different climatic periods throughout the Holocene. Along with biological proxies, XRF and sedimentological data were used to infer catchment-related and lake-internal geochemical changes. Both biological and geochemical data complement each other and support the assignment of the following lake developmental stages of Lake Satagay: initial lake formation during the deglacial, lake deepening caused by rising temperatures in the Early Holocene, lake shallowing and high productivity during the Mid-Holocene, and stable shallow conditions during the cooler Late Holocene. The lake developmental stages coincide with known alaas stages and suggest that Lake Satagay has not yet reached the final stage of alaas lake development.

Rising temperatures, recent anthropogenic impact and artificial draining of the lake might, however, accelerate desiccation. Eventually, this may lead to the loss of Lake Satagay and thus an important freshwater source for the local population, while being unable to serve as an agricultural alaas for

haymaking and livestock farming. Since rapidly changing environmental conditions currently affect the whole boreal zone, many more alaas lakes may be experiencing similar developments. To sustain these landscapes for the local communities, it is important to understand long-term lake development in similar lake systems to allow better future management of these unique lake types.

Data availability The sedaDNA metabarcoding data presented in this study is published in the Dryad database (Baisheva et al. 2022a). The diatom and biogeochemical composition of the sediment core is published in the PANGAEA repository (Baisheva et al. 2022b).

Declarations

Conflict of interest The authors declare no competing interests.

References

Alsos IG, Lammers Y, Yoccoz NG, Jørgensen T, Sjögren P, Gielly L, Edwards ME (2018) Plant DNA metabarcoding of lake sediments: how does it represent the contemporary vegetation? PLoS ONE 13(4):e0195403. https://doi.org/10.1371/journal.pone.0195403

Andreev A (2000) History of vegetation and climate of Central Yakutia during the Late Pleistocene and Holocene. In: Proceedings of the international conference ''Lakes of cold regions'', Part IV. Paleoclimatology, Paleolimnology and Paleoecology Issue. Yakutsk, Russia, (in Russian).

Andreev A, Klimanov V, Sulerzhitskiy L (1992) Vegetation and climate history of central Yakutia during the last 11.000 years. In: Conference: geochronology of quaternary conference proceedings. pp 112–117

Baisheva I, Pestryakova L, Glückler R, Herzschuh U, Stoof-Leichsenring KR (2022a) Diatoms and plants sedimentary ancient DNA from Lake Satagay (Central Yakutia, Siberia) covering the last 10,800 years. Dryad Dataset. https://doi.org/10.5061/dryad.vq83bk3w5

Baisheva I, Pestryakova L, Levina S, Glückler R, Biskaborn BK, Vyse SA, Heim B, Herzschuh U, Stoof-Leichsenring KR (2022) Diatom- and biogeochemical composition of the sediment core EN18224-4 from Lake Satagay, Central Yakutia, Siberia. PANGAEA. https://doi.org/10.1594/PANGAEA.948331

Battarbee RW, Jones VJ, Flower RJ, Cameron NG, Bennion H, Carvalho L, Juggins S (2001) Diatoms. In: Smol JP, Birks HJB, Last WM (eds) Tracking environmental change using lake sediments, vol 3. Terrestrial, Algal, and Siliceous Indicators. Kluwer, Dordrecht, pp 155–202

Biskaborn BK, Herzschuh U, Bolshiyanov D, Savelieva L, Diekmann B (2012) Environmental variability in Northeastern Siberia during the last ~ 13,300 yr inferred from lake diatoms and sediment–geochemical parameters. Palaeogeogr, Palaeoclimatol, Palaeoecol 329–330:22–36. https://doi.org/10.1016/j.palaeo.2012.02.003

Biskaborn BK, Herzschuh U, Bolshiyanov D, Savelieva L, Zibulski R, Diekmann B (2013) Late Holocene thermokarst variability inferred from diatoms in a lake sediment record from the Lena Delta. Siberian Arctic J Paleolimnol 49(2):155–170. https://doi.org/10.1007/s10933-012-9650-1

Biskaborn BK, Subetto DA, Savelieva LA, Vakhrameeva PS, Hansche A, Herzschuh U, Klemm J, Heinecke L, Pestryakova LA, Meyer H, Kuhn G, Diekmann B (2016) Late quaternary vegetation and lake system dynamics in north-eastern Siberia: implications for seasonal climate variability. Quat Sci Rev 147:406–421. https://doi.org/10.1016/j.quascirev.2015.08.014

Biskaborn BK, Smith SL, Noetzli J, Matthes H, Vieira G, Streletskiy DA, Schoeneich P, Romanovsky VE, Lewkowicz AG, Abramov A, Allard M, Boike J, Cable WL, Christiansen HH, Delaloye R, Diekmann B, Drozdov D, Etzelmüller B, Grosse G, Guglielmin M, Ingeman-Nielsen T, Isaksen K, Ishikawa M, Johansson M, Johannsson H, Joo A, Kaverin D, Kholodov A, Konstantinov P, Kröger T, Lambiel C, Lanckman J-P, Luo D, Malkova G, Meiklejohn I, Moskalenko N, Oliva M, Phillips M, Ramos M, Sannel ABK, Sergeev D, Seybold C, Skryabin P, Vasiliev A, Wu Q, Yoshikawa K, Zheleznyak M, Lantuit H (2019) Permafrost is warming at a global scale. Nat Commun 10(1):264. https://doi.org/10.1038/s41467-018-08240-4

Biskaborn BK, Nazarova L, Kröger T, Pestryakova LA, Syrykh L, Pfalz G, Herzschuh U, Diekmann B (2021) Late Quaternary climate reconstruction and lead-lag relationships of biotic and sediment-geochemical indicators at Lake Bolshoe Toko, Siberia. Front Earth Sci 9:737353. https://doi.org/10.3389/feart.2021.737353

Bosikov NP (1991) Alaas evolution of central Yakutia. Permafrost Institute SD USSR AS, Yakutsk, p 128

Bouchard F, Francus P, Pienitz R, Laurion I (2011) Sedimentology and geochemistry of thermokarst ponds in discontinuous permafrost, subarctic Quebec. Can J Geophys Res 116:G0M04. https://doi.org/10.1029/2011JG001675

Boyer F, Mercier C, Bonin A, Le Bras Y, Taberlet P, Coissac E (2015) OBITOOLS: a unix-inspired software package for DNA metabarcoding. Mol Ecol Res 16:176–182. https://doi.org/10.1111/1755-0998.12428

Crate S, Ulrich M, Habeck JO, Desyatkin AR, Desyatkin RV, Fedorov AN, Hiyama T, Iijima Y, Ksenofontov S, Mészáros C, Takakura H (2017) Permafrost livelihoods: a transdisciplinary review and analysis of thermokarst-based systems of indigenous land use. Anthropocene 18:89–104. https://doi.org/10.1016/j.ancene.2017.06.001

Desyatkin RV (2004) Water resources of taiga-alas landscapes in Central Yakutia and problems of water supply for the population. In: The 6th international GAME conference material

Desyatkin RV, Filippov N, Desyatkin A, Konyushkov D, Goryachkin S (2021) Degradation of arable soils in central Yakutia: negative consequences of global warming for Yedoma landscapes. Front Earth Sci 9:683730. https://doi.org/10.3389/feart.2021.683730

Duff KE, Laing TE, Smol JP, Lean DRS (1998) Limnological characteristics of lakes located across arctic treeline in northern Russia. Hydrobiologia 391:203–220. https://doi.org/10.1023/A:1003542322519

Dulias K, Stoof-Leichsenring KR, Pestryakova LA, Herzschuh U (2017) Sedimentary DNA versus morphology in the analysis of diatom-environment relationships. J Paleolimnol 57:51–66. https://doi.org/10.1007/s10933-016-9926-y

Fedorov AN (2022) Permafrost landscape research in the northeast of Eurasia. Earth 3(1):460–478. https://doi.org/10.3390/earth3010028

Fedorov A, Vasilyev N, Torgovkin Y, Shestakova A, Varlamov S, Zheleznyak M, Shepelev V, Konstantinov P, Kalinicheva S, Basharin N, Makarov V, Ugarov I, Efremov P, Argunov R, Egorova L, Samsonova V, Shepelev A, Vasiliev A, Ivanova R, Galanin A, Lytkin V, Kuzmin G, Kunitsky V (2018) Permafrost-landscape map of the Republic of Sakha (Yakutia) on a scale 1:1,500,000. Geosciences 8(12):465. https://doi.org/10.3390/geosciences8120465

Fietz S, Bleiss W, Hepperle D, Koppitz H, Krienitz L, Nicklisch A (2005) First record of Nannochloropsis limnetica (Eustigmatophyceae) in the autotrophic picoplankton from Lake Baikal. J Phycol 41:780–790. https://doi.org/10.1111/j.1529-8817.2005.00112.x

Glückler R, Geng R, Grimm L, Baisheva I, Herzschuh U, Stoof-Leichsenring KR, Kruse S, Andreev A, Pestryakova L, Dietze E (2022) Holocene wildfire and vegetation dynamics in Central Yakutia, Siberia, reconstructed from lake-sediment proxies. Front Ecol Evol 10:962906. https://doi.org/10.3389/fevo.2022.962906

Gross EM, Erhard D, Iványi E (2003) Allelopathic activity of Ceratophyllum demersum L. and Najas marina ssp. intermedia (Wolfgang) Casper. Hydrobiologia 506–509(1–3):583–589. https://doi.org/10.1023/B:HYDR.0000008539.32622.91

Herzschuh U, Mischke S, Meyer H, Plessen B, Zhang C (2010) Lake nutrient variability inferred from elemental (C, N, S) and isotopic (δ13C, δ15N) analyses of aquatic plant macrofossils. Quat Sci Rev 29(17–18):2161–2172. https://doi.org/10.1016/j.quascirev.2010.05.011

Herzschuh U, Pestryakova LA, Savelieva LA, Heinecke L, Böhmer T, Biskaborn BK, Andreev A, Ramisch A, Shinneman ALC, Birks HJB (2013) Siberian larch forests and the ion content of thaw lakes form a geochemically functional entity. Nat Commun 4(1):2408. https://doi.org/10.1038/ncomms3408

Huang S, Herzschuh U, Pestryakova LA, Zimmermann HH, Davydova P, Biskaborn BK, Shevtsova I, Stoof-Leichsenring KR (2020) Genetic and morphologic determination of diatom community composition in surface sediments from glacial and thermokarst lakes in the Siberian Arctic. J Paleolimnol 64:225–242. https://doi.org/10.1007/s10933-020-00133-1

Jones BM, Grosse G, Arp CD, Miller E, Liu L, Hayes DJ, Larsen CF (2015) Recent Arctic tundra fire initiates widespread thermokarst development. Sci Rep 5:15865. https://doi.org/10.1038/srep15865

Juggins S (2019) rioja: analysis of quaternary science data. http://cran.r-project.org/web/packages/rioja/index.html

Kipriyanova LM, Dolmatova LA, Bazarova BB, Naydanov BB, Romanov RE, Tsybekmitova GT, Dyachenko AV (2017) On the ecology of some species of genus Stuckenia (Potamogetonaceae) in lakes of Zabaykalsky Krai and the Republic of Buryatia. Inland Water Biol 10(1):73–82. https://doi.org/10.1134/S1995082917010096

Krammer K, Lange-Bertalot H (1986–1991) Bacillariophyceae. Süsswasserflora von Mitteleuropa. Band 2, teil 1–4.

(Bacillariophyceae. Freshwater flora of central Europe. Vol. 2, parts 1–4.) Gustav Fischer Verlag, Stuttgart

Krienitz L, Hepperle D, Stich HB, Weiler W (2000) *Nannochloropsis limnetica* (Eustigmatophyceae), a new species of picoplankton from freshwater. Phycologia 39(3):219–227. https://doi.org/10.2216/i0031-8884-39-3-219.1

Kruse S, Bolshiyanov D, Grigoriev MN, Morgenstern A, Pestryakova L, Tsibizov L et al (2019) Russian-German cooperation: expeditions to Siberia in 2018. Rep Polar Mar Res Group 734:1–257. https://doi.org/10.2312/BzPM_0734_2019

Kumke T, Ksenofontova M, Pestryakova L, Nazarova L, Hubberten HW (2007) Limnological characteristics of lakes in the lowlands of central Yakutia. Russia J Limnol 66(1):40. https://doi.org/10.4081/jlimnol.2007.40

Lange-Bertalot H (1993) 85 Neue taxa und uber 100 weitere neu definierte Taxa erganzend zur Subwasserflora von Mittleuropa Bibliotheca Diatomologica 27, 454 p. Cramer, Berlin, Stuttgart

Lange-Bertalot H, Metzeltin D (1996) Indicators of oligotrophy. Iconogr Diatomol 2:390

Liu S, Stoof-Leichsenring KR, Kruse S, Pestryakova LA, Herzschuh U (2020) Holocene vegetation and plant diversity changes in the north-eastern Siberian treeline region from pollen and sedimentary ancient DNA. Front Ecol Evo 8:560243. https://doi.org/10.3389/fevo.2020.560243

Marzetz V, Koussoroplis AM, Martin-Creuzburg D, Striebel M, Wacker A (2017) Linking primary producer diversity and food quality effects on herbivores: a biochemical perspective. Sci Rep 7(1):11035. https://doi.org/10.1038/s41598-017-11183-3

Meyers PA, Lallier-Vergès E (1999) Lacustrine sedimentary organic matter records of late Quaternary paleoclimates. J Paleolimnol 21:345–372. https://doi.org/10.1023/A:1008073732192

Meyers PA, Teranes JL (2002) Sediment organic matter. In: Last WM, Smol JP (eds) Tracking environmental change using lake sediments, physical and geochemical methods, vol 2. Kluwer Academic Publishers, Dordrecht, pp 239–269. https://doi.org/10.1007/0-306-47670-3_9

Müller S, Tarasov P, Andreev A, Diekmann B (2009) Late Glacial to Holocene environments in the present-day coldest region of the Northern Hemisphere inferred from a pollen record of Lake Billyakh, Verkhoyansk Mts, NE Siberia. Clim past 5:73–84. https://doi.org/10.5194/cp-5-73-2009

Nazarova L, Lüpfert H, Subetto D, Pestryakova L, Diekmann B (2013) Holocene climate conditions in central Yakutia (eastern Siberia) inferred from sediment composition and fossil chironomids of Lake Temje. Quat Int 290–291:264–274. https://doi.org/10.1016/j.quaint.2012.11.006

Oksanen J, Blanchet FG, Kindt R, Legendre P, Minchin P, O'Hara B, Simpson G, Solymos P, Stevens H, Wagner H (2015) Vegan: community ecology package. R Package Version 2.2–1. 2. 1–2.

Palagushkina OV, Nazarova LB, Wetterich S, Schirrmeister L (2012) Diatoms of modern bottom sediments in Siberian Arctic. Contemp Probl Ecol 5(4):413–422. https://doi.org/10.1134/S1995425512040105

Pedersen MW, Overballe-Petersen S, Ermini L, Sarkissian CD, Haile J, Hellstrom M, Spens J, Thomsen PF, Bohmann K, Cappellini E, Schnell IB, Wales NA, Carøe C, Campos

PF, Schmidt AMZ, Gilbert MTP, Hansen AJ, Orlando L, Willerslev E (2015) Ancient and modern environmental DNA. Phil Trans R Soc B 370(1660):20130383. https://doi.org/10.1098/rstb.2013.0383

Pestryakova LA, Herzschuh U, Wetterich S, Ulrich M (2012) Present-day variability and Holocene dynamics of permafrost-affected lakes in central Yakutia (eastern Siberia) inferred from diatom records. Quat Sci Rev 51:56–70. https://doi.org/10.1016/j.quascirev.2012.06.020

Pestryakova LA, Nikolaev AN, Subetto DA, Frolova LA, Bobrov AA, Gorodnichev RM (2016) Paleoecology. Methodological basics of paleoecology: tutorial. North-Eastern Federal University Publishing House, Yakutsk, p 84

Pestryakova LA, Herzschuh U, Gorodnichev R, Wetterich S (2018) The sensitivity of diatom taxa from Yakutian lakes (north-eastern Siberia) to electrical conductivity and other environmental variables. Polar Res 37(1):1485625. https://doi.org/10.1080/17518369.2018.1485625

Pienitz R, Smol JP (1993) Diatom assemblages and their relationship to environmental variables in lakes from the boreal forest-tundra ecotone near Yellowknife, Northwest Territories, Canada. Hydrobiol 269:391–404. https://doi.org/10.1007/BF00028037R

R Core Team (2019) R: a language and environment for statistical computing. https://www.r-project.org

Rott E, Duthie HC, Pipp E (1998) Monitoring organic pollution and eutrophication in the Grand River, Ontario, by means of diatoms. Can J Fish Aquat Sci 55:1443–1453. https://doi.org/10.1139/f98-038

Saulnier-Talbot É, Pienitz R, Vincent WF (2003) Holocene lake succession and palaeo-optics of a Subarctic lake, northern Québec, Canada. Holocene 13(4):517–526. https://doi.org/10.1191/0959683603hl641rp

Séjourné A, Costard F, Fedorov A, Gargani J, Skorve J, Massé M, Mège D (2015) Evolution of the banks of thermokarst lakes in central Yakutia (central Siberia) due to retrogressive thaw slump activity controlled by insolation. Geomorphology 241:31–40. https://doi.org/10.1016/j.geomorph.2015.03.033

Soininen EM, Gauthier G, Bilodeau F, Berteaux D, Gielly L, Taberlet P, Gussarova G, Bellemain E, Hassel K, Stenøien HK, Epp L, Schrøder-Nielsen A, Brochmann C, Yoccoz NG (2015) Highly overlapping winter diet in two sympatric lemming species revealed by DNA metabarcoding. PLoS ONE 10(1):e0115335. https://doi.org/10.1371/journal.pone.0115335

Soloviev PA (1959) The cryolithozone of northern part of the lena-amga interfluve. Academy of Sciences, Moscow

Sønstebø JH, Gielly L, Brysting AK, Elven R, Edwards M, Haile J, Willerslev E, Coissac E, Rioux D, Sannier J, Taberlet P, Brochmann C (2010) Using next-generation sequencing for molecular reconstruction of past Arctic vegetation and climate. Mol Ecol Resour 10:1009–1018. https://doi.org/10.1111/j.1755-0998.2010.02855.x

Stoof-Leichsenring K, Epp L, Trauth M, Tiedemann R (2012) Hidden diversity in diatoms of Kenyan Lake Naivasha: a genetic approach detects temporal variation. Mol Ecol 21:1918–1930. https://doi.org/10.1111/j.1365-294X.2011.05412.x

Stoof-Leichsenring KR, Dulias K, Biskaborn BK, Pestryakova LA, Herzschuh U (2020) Lake-depth related pattern of genetic and morphological diatom diversity in boreal lake Bolshoe Toko, eastern Siberia. PLoS ONE 15(4):e0230284. https://doi.org/10.1371/journal.pone.0230284

Stoof-Leichsenring KR, Huang S, Liu S, Jia W, Li K, Liu X, Pestryakova LA, Herzschuh U (2022) Sedimentary DNA identifies modern and past macrophyte diversity and its environmental drivers in high-latitude and high-elevation lakes in Siberia and China. Limnol Oceanogr 67(5):1126–1141. https://doi.org/10.1002/lno.12061

Taberlet P, Coissac E, Pompanon F, Gielly L, Miquel C, Valentini A, Vermat T, Corthier G, Brochmann C, Willerslev E (2007) Power and limitations of the chloroplast TrnL (UAA) intron for plant DNA barcoding. Nucleic Acids Res 35(3):e14–e14. https://doi.org/10.1093/nar/gkl938

Ulrich M, Wetterich S, Rudaya N, Frolova L, Schmidt J, Siegert C, Fedorov AN, Zielhofer C (2017) Rapid thermokarst evolution during the mid-Holocene in central Yakutia. Russia Holocene 27(12):1899–1913. https://doi.org/10.1177/0959683617708454

van den Boogaart KG, Tolosana-Delgado R (2006) Compositional data analysis with 'R' and the package 'compositions.' In: Buccianti A, Mateu-Figueras G, Pawlowsky-Glahn V (eds) Compositional data analysis in the geosciences: from theory to practice, vol 264. Geological Society of London Special Publication, London, pp 119–127

van Donk E, Kilham SS (1990) Temperature effects on silicon- and phosphorus-limited growth and competitive interactions among three diatoms. J Phycol 26:40–50

Vyse SA, Herzschuh U, Andreev AA, Pestryakova LA, Diekmann B, Armitage SJ, Biskaborn BK (2020) Geochemical and sedimentological responses of Arctic glacial Lake Ilirney, Chukotka (Far East Russia) to palaeoenvironmental change since ~51.8 ka BP. Quat Sci Rev 247:106607. https://doi.org/10.1016/j.quascirev.2020.106607

Walker MJC, Berkelhammer M, Björck S, Cwynar LC, Fisher DA, Long AJ, Lowe JJ, Newnham RM, Rasmussen SO, Weiss H (2012) Formal subdivision of the Holocene Series/Epoch: a Discussion paper by a working group of INTIMATE (Integration of ice-core, marine and terrestrial records) and the subcommission on quaternary stratigraphy (international commission on stratigraphy). J Quaternary Sci 27:649–659. https://doi.org/10.1002/jqs.2565

Willerslev E, Davison J, Moora M, Zobel M, Coissac E, Edwards ME, Lorenzen ED, Vestergård M, Gussarova G, Haile J, Craine J, Gielly L, Boessenkool S, Epp LS, Pearman PB, Cheddadi R, Murray D, Bråthen KA, Yoccoz N, Binney H, Cruaud C, Wincker P, Goslar T, Alsos IG, Bellemain E, Brysting AK, Elven R, Sønstebø JH, Murton J, Sher A, Rasmussen M, Rønn R, Mourier T, Cooper A, Austin J, Möller P, Froese D, Zazula G, Pompanon F, Rioux D, Niderkorn V, Tikhonov A, Savvinov G, Roberts RG, MacPhee RDE, Gilbert MTP, Kjær KH, Orlando L, Brochmann C, Taberlet P (2014) Fifty thousand years of Arctic vegetation and megafaunal diet. Nature 506(7486):47–51. https://doi.org/10.1038/nature12921

Zakharova EA, Kouraev AV, Stephane G, Franck G, Desyatkin RV, Desyatkin AR (2018) Recent dynamics of hydro-ecosystems in thermokarst depressions in central Siberia from satellite and in situ observations: importance for agriculture and human life. Sci Total Environ 615:1290–1304. https://doi.org/10.1016/j.scitotenv.2017.09.059

Zhao Y, Liang C, Cui Q, Qin F, Zheng Z, Xiao X, Ma C, Felde VA, Liu Y, Li Q, Zhang Z, Herzschuh U, Xu Q, Wei H, Cai M, Cao X, Guo Z, Birks HJB (2021) Temperature reconstructions for the last 1.74-Ma on the eastern Tibetan Plateau based on a novel pollen-based quantitative method. Glob Planet Change 199:103433. https://doi.org/10.1016/j.gloplacha.2021.103433